Hindawi Publishing Corporation
EURASIP Journal on Wireless Communications and Networking
Volume 2010, Article ID 398401, 12 pages
doi:10.1155/2010/398401

Research Article

Time Reversal UWB Communication System: A Novel Modulation Scheme with Experimental Validation

I. H. Naqvi,[1] A. Khaleghi,[2] and G. El Zein[3]

[1] *LUMS School of Science and Engineering, Sector U, DHA, 54792 Lahore Cantt, Pakistan*
[2] *EE Department, Khaje Nasir Toosi University (KNTU), Tehran, Iran*
[3] *Institute of Electronics and Telecommunications of Rennes, IETR-UMR CNRS 6164, INSA, 20 Avenue des Buttes de Coesmes, 35043 Rennes, France*

Correspondence should be addressed to I. H. Naqvi, ijaznaqvi@lums.edu.pk

Received 3 August 2009; Accepted 18 February 2010

Academic Editor: Thushara Abhayapala

A new modulation scheme is proposed for a time reversal (TR) ultra wide-band (UWB) communication system. The new modulation scheme uses the binary pulse amplitude modulation (BPAM) and adds a new level of modulation to increase the data rate of a TR UWB communication system. Multiple data bits can be transmitted simultaneously with a cost of little added interference. Bit error rate (BER) performance and the maximum achievable data rate of the new modulation scheme are theoretically analyzed. Two separate measurement campaigns are carried out to analyze the proposed modulation scheme. In the first campaign, the frequency responses of a typical indoor channel are measured and the performance is studied by the simulations using the measured frequency responses. Theoretical and the simulative performances are in strong agreement with each other. Furthermore, the BER performance of the proposed modulation scheme is compared with the performance of existing modulation schemes. It is shown that the proposed modulation scheme outperforms QAM and PAM for $M \geq 4$ in an AWGN channel. In the second campaign, an experimental validation of the proposed modulation scheme is done. It is shown that the performances with the two measurement campaigns are in good agreement.

1. Introduction

One of the biggest strengths of the UWB technology is derived by its ultra large bandwidth. Owning to such a large bandwidth, UWB systems can attain very high data rates. UWB technology is opening the doors for a range of new applications as well as complementing existing wireless systems. The ability of pulse-based UWB to resolve individual multipath components is exploited in the recent research for short range communication applications. However, large number of resolvable paths and low power limitations necessitate a complex receiver system. To collect the received signal energy, Rake receiver, transmit-reference, or the decision feedback autocorrelation receiver can be implied [1–3]. Each technique has its own difficulties and drawbacks. Time Reversal (TR) has been proposed as a technique to shift the design complexity from the receiver to the transmitter. Classically, TR has been applied in acoustics and under water communication applications [4, 5], but recently, it has been widely studied for UWB communications [6–16]. The received signal in a TR system is considerably focused in spatial and temporal domains and can be received using simple energy threshold detectors.

This paper proposes a novel modulation scheme which improves the data rate by spreading the transmitted data in a given large bandwidth, over the delay time. This scheme has been submitted in one of the patents submitted by IETR [17]. Multiple data bits are packed in one time slot to add a new level of modulation along with the BPAM modulation. The packed data bits have quasi-orthogonal waveforms and they cause minimum interference to the other bits. Thus, the received bits can be distinguished and demodulated quite easily. The BER performance of the new modulation scheme and the maximum achievable data rate are theoretically analyzed. Two separate measurement campaigns are carried out to analyze the performance of the modulation scheme. TR communication is simulated using the measurement results of the first measurement campaign. The simulated

and the theoretical results are compared to each other. Furthermore, the performance of the new modulation scheme is compared with the performance of the quadrature amplitude modulation (QAM) and the pulse amplitude modulation (PAM) in an AWGN channel. With the second measurement campaign, the new modulation scheme is experimentally validated using time domain instruments. The performance of the proposed modulation scheme is compared for the two measurement campaigns.

The rest of the paper is organized as follows. A brief introduction of the time reversal is presented in Section 2. The modulation principle of the proposed scheme, theoretical performance, and the analysis of the maximum achievable data rate is presented in Section 3. Experimental setup along with the simulated and measurement results of BER performance are presented and analyzed in Section 4. Finally, Section 5 concludes this paper.

2. Time Reversal

Time reversal (TR) is a transmission scheme in which a time reversed channel impulse response (CIR) is used as a transmitter prefilter. In a first step, the CIR is estimated between a transmitter and a receiver. Then the CIR is flipped in time and emitted by the transmitter. The time reversed wave back propagates in the channel following the same paths as the CIR's ones but in the reverse order. Finally at the receiver, all the paths add up coherently in the time and spatial domains. For dense multipath propagation channels, strong temporal compression, and high spatial focusing can be achieved with a focusing gain of about 8 dB [14]. For communication purposes, this gain improves, for instance, the transmission range. Inter Symbol Interference (ISI) effects are mitigated by temporal compression and multiuser interference is reduced due to spatial focusing. The received signal ($y_j(t)$) at the intended receiver (j) can be mathematically represented as

$$y_j(t) = s(t) \star h_{ij}(-t) \star h_{ij}(t) = s(t) \star R_{ij}^{\text{auto}}(t), \quad (1)$$

where $h_{ij}(t)$ is the CIR from the transmitting point (i) to an intended receiver (j), $s(t)$ is the transmitted signal, $\star$ denotes convolution product, and $R_{ij}^{\text{auto}}(t)$ is the autocorrelation of the CIR, $h_{ij}(t)$. The received signal at any nonintended receiver (k) is written as

$$y_k(t) = s(t) \star h_{ij}(-t) \star h_{ik}(t) = s(t) \star R_{ikj}^{\text{cross}}(t), \quad (2)$$

where $h_{ik}(t)$ is the CIR from the transmitting point (i) to an unintended receiver (k) and $R_{ikj}^{\text{cross}}(t)$ is the cross-correlation of the CIR $h_{ik}(t)$ and $h_{ij}(t)$. If the channels are uncorrelated, then the signal transmitted for one receiver will act as a noise for a receiver at any other location. Thus, a secure communication is achieved with low probability of detection and low probability of interception.

In the practical implementation of the TR systems, the precoding filter is truncated in time to reduce the filter length and thus the system complexity. The truncated response is represented as $h'(-t)$. For data communication purpose, the transmitted symbols are modulated by binary pulse amplitude modulation (BPAM) scheme. The kth symbol, d_k, of the symbol sequence is equal to 1 or -1 for the data bits 1 or 0, respectively. Therefore, the received signal at the intended receiver is written as

$$\begin{aligned} y(t) &= \underbrace{A\sum_k d_k h'(-t - kT_s)}_{\text{Transmitted RF signal}} \star \underbrace{h(t)}_{\text{CIR}} + n(t) \\ &\approx A\sum_k d_k R'_{hh}(t - kT_s) + n(t), \end{aligned} \quad (3)$$

where A is a normalization factor, T_s is the intersymbol interval, $n(t)$ is the noise, and $R'_{hh}(t)$ is the correlation between the truncated CIR ($h'(t)$) and the original CIR ($h(t)$). For the sake of simplicity, we have supposed that the T_s is equal to the length of the measured time reversed CIR ($h'(-t)$). As the amplitude of the peak of the received signal is proportional to the energy of the transmitted signal ($\int h'^2 dt$), the truncation process decreases the peak of the received signal. Due to BPAM, the polarity of the received signal peaks depends on the transmitted data bit and is used for the detection of the data bits.

3. Description of the Novel Modulation Scheme

This paper presents an original technique for data modulation for time reversal systems. We keep the BPAM modulation concept and add a second modulation level for the transmitted data. Let the CIR of the communication channel be represented by the classic tapped delay line model:

$$h(t) = \sum_{i=0}^{N-1} \alpha_i \delta(t - \tau_i), \quad (4)$$

where $\delta(t)$ is the Dirac's delta function, N is the total number of taps in the CIR, and τ_i is the delay associated to the ith tap.

3.1. The Modulation Principle. In the proposed scheme, the data bits (d_k) which are the antipodal binary bits (± 1) are divided into m-parallel lines using serial-to-parallel (S/P) conversion unit and then passed through multiple filter banks, $\{K_1(t), K_2(t), \ldots, K_m(t)\}$, where m is the number of bits transmitted in parallel giving us a modulation order $M = 2^m$.

Figure 1 shows the conceptual block diagram of the new modulation scheme. The response of each filter is the shifted and truncated version of the original filter response $h'(-t)$. Let the measured, truncated, and time reversed CIR be represented as $h'(-t)$ and has a length $L \leq N$ taps:

$$h'(-t) = \sum_{i=0}^{L-1} a_i \delta(t - i\tau_s), \quad (5)$$

where L is the total number of the time reversal filter components having an equivalent length of $T_{\text{sig}} = L\tau_s$ in time (seconds), a_i is the associated amplitude, and $i\tau_s$ is the

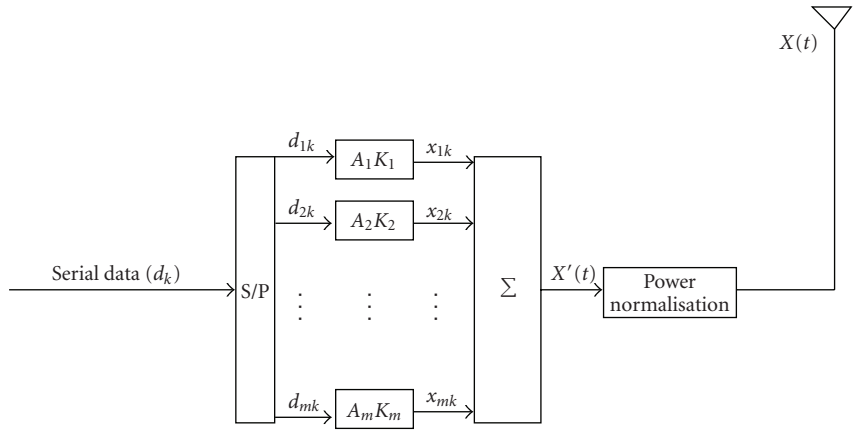

Figure 1: Conceptual block diagram of the new modulation scheme.

associated delay of the multipath components. The duration, τ_s, is the time between two consecutive samples and depends on the maximum sampling rate of the time reversal filter. For instance, if the measured CIR is sampled with a sampling rate of 5 GS/s, the delay of $\tau_s = 0.2$ ns is obtained between two consecutive samples; therefore, the number of taps (L) in filter having a length of 50 ns is $L = 250$ samples or taps. The responses of the filter banks are produced by shifting $h'(-t)$ to either left or right and then forcing the shifted part to zero so that the shifted signal can be packed in the same signal duration. Figure 2 shows the pattern of the left or right shift of $l = 1; 2$ taps. As shown for the left shift of 1 tap, the last three taps are shifted to left by one tap and the slot for last tap is filled with zero. For the right shift of 1 tap, first three taps are shifted to right and then the slot for the first tap is filled with zero. If $h'(-t)$ is shifted left or right by $T_b = l_{\text{opt}}\tau_s$, the expression is given by

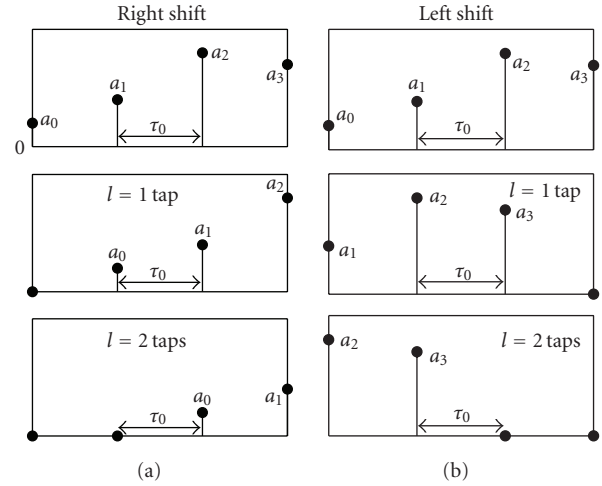

Figure 2: Pattern for the left and right shifts.

$$\begin{aligned}
&\text{right shift}(h'(-t, T_b)) = \widehat{h}(-t - T_b)\\
&= \left[\text{zeros}\left(1, l_{\text{opt}}\right) \sum_{i=1}^{L-l_{\text{opt}}} a_i \delta\left(t - \left(l_{\text{opt}} + i\right)\tau_{\text{s}}\right)\right],\\
&\text{left shift}(h'(-t), T_b) = \widehat{h}(-t + T_b)\\
&= \left[\sum_{i=1}^{L-l_{\text{opt}}} a_i + l_{\text{opt}}\delta(t - i\tau_{\text{s}})\text{zeros}\left(1, l_{\text{opt}}\right)\right],
\end{aligned} \tag{6}$$

where $\text{zeros}(1; l_{\text{opt}})$ is a vector containing l_{opt} number of zeros, $l_{\text{opt}}(T_b/\tau_s)$ is the number of shifted taps required to exercise a shift of T_b, and a_i is the coefficient of $h'(-t)$ at the delay $i\tau_s$. Note that $\widehat{h}_j(-t - T_b)$ has $L - l_{\text{opt}}$ nonzero taps. As we have used only left shift for the new modulation scheme, the response of the ith filter bank becomes $K_i(t) = \widehat{h}(-t+iT_b)$ with $i \in \{0, \ldots, m-1\}$.

The signals after passing through the filter banks are then normalized to equal power and added together giving a waveform which can be written as

$$X'(t) = \sum_{i=0}^{m-1} d_i A_i \widehat{h}(-t + iT_b), \tag{7}$$

where the normalization factor A_i is given by the expression:

$$A_i = \frac{1}{\sqrt{\left\|\widehat{h}(-t + iT_b)\right\|^2}}, \tag{8}$$

where $\|\cdot\|$ is the Frobenius norm operation. The normalization insures that each of the transmitted bits has equal power.

Due to addition of the signals, the power of the resulted waveform, $X'(t)$, is modified. To keep a constant transmitted power (P_0) with the transmitter unit of the communication system, the signal $X'(t)$ must be renormalized. This power normalization allows the system to respect the transmit power regulations. In order to normalize the total transmit power to P_0, each bit is transmitted with a power of P_0/m resulting in a power of P_0 in a time frame, and periodic transmission of the frames is done with a period of $T_s = T_{\text{sig}}$.

The resulting transmitted signal can be expressed as

$$X(t) = \sum_k \frac{1}{\sqrt{m}} X'(t - kT_s) = \sum_k \frac{1}{\sqrt{m}} \sum_{i=0}^{m-1} d_{ik} A_i \hat{h}(-t + iT_b - kT_s). \tag{9}$$

The signal $X(t)$ is transmitted in the propagation channel. The received signal can be written as

$$R_x(t) = h(t) \star X(t) + n(t) = h(t) \star \sum_k \frac{1}{\sqrt{m}} \sum_{i=0}^{m-1} d_{ik} A_i \hat{h}(-t + iT_b - kT_s) + n(t) = \sum_k \sum_{i=0}^{m-1} d_{ik} w_{rx_i}(t + iT_b - kT_s) + n(t), \tag{10}$$

where $w_{rx_i}(t + iT_b - kT_s) = h(t) \star \hat{h}(-t + iT_b - kT_s)$ is the received signal waveform for the ith bit. Now if the channel delay spread is T_d, the received signal peak will be detected at $t_{\text{peak}} = T_d + T_s$. If m bits are transmitted simultaneously, peaks can be detected at: $t_{\text{peak}_i} = t_{\text{peak}} + iT_b$, for all $i \in \{0, \ldots, m-1\}$. Assuming a perfect synchronization, the received peaks for the ith bit can be written as

$$R_x\left(t_{\text{peak}_i}\right) = \sum_k \left(\underbrace{d_{ik} w_{rx_i}\left(t_{\text{peak}} + iT_b - kT_s\right)}_{\text{signal}} + \underbrace{\sum_{j=0, j\neq i}^{m-1} d_{jk} w_{rx_j}\left(t_{\text{peak}} + iT_b - kT_s\right)}_{\text{Intra Symbol Interference}} \right) + n(t). \tag{11}$$

The vectorial form for the kth symbol can be written as

$$\vec{z_k} = \vec{d_k} W_{rx} + \vec{\eta_k}, \tag{12}$$

where $\vec{z_k}$ is the decision variable, $\vec{d_k} = (d_{0k}, \ldots, d_{m-1k})$ is a vector of m transmitted bits in the kth symbol, $\vec{\eta_k}$ is the noise vector, and the matrix W_{rx} is defined as

$$W_{rx} = \begin{pmatrix} w_{0,0} & w_{0,1} & \cdots & w_{0,m-1} \\ w_{1,0} & w_{1,1} & \cdots & w_{1,m-1} \\ \vdots & \vdots & \ddots & \vdots \\ w_{m-1,0} & w_{m-1,1} & \cdots & w_{m-1,m-1} \end{pmatrix}, \tag{13}$$

where $w_{x,y} = w_{rx_x}(t_{\text{peak}} + yT_b - kT_S)$ with diagonal as the peaks of the Signal and the rest are the interference peaks.

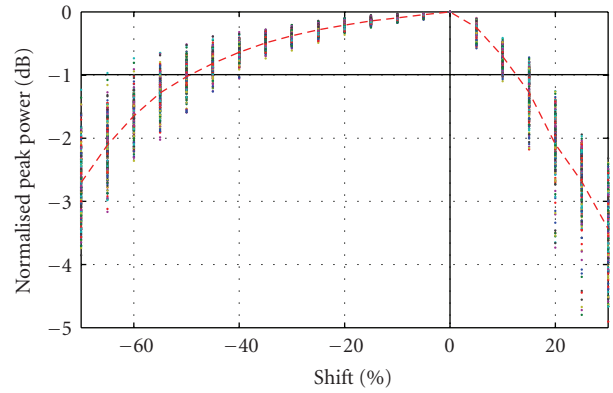

Figure 3: Received signal peak power with left and right shifts normalized to the peak with no shift.

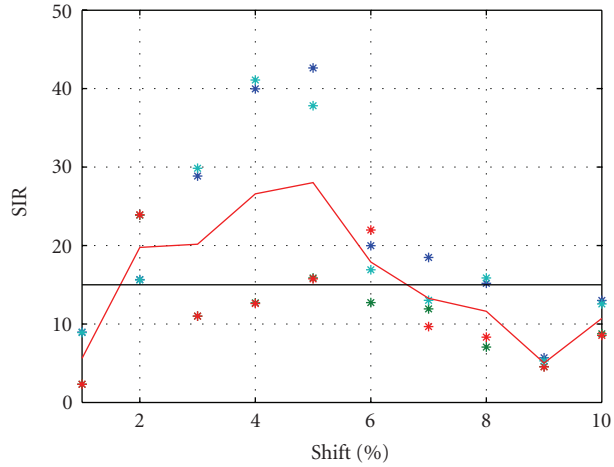

Figure 4: Average and bit by bit signal to interference ratio for the received signal with 4 simultaneous bits ($m = 4$) with different shift steps (in percentage of the transmitted signal length (T_{sig})).

3.2. Effects of Shift on the Received Signal. In a TR communication system, as the received signal is the auto correlation function of the CIR, the received signal peak is the sum of the square of the coefficients of CIR (from the properties of auto correlation function). The transmitted signal for the new modulation scheme is given by (9). The received signal at the peak is given by (11). Neglecting the interference and the noise, the received signal peak for the jth bit of the kth symbol is written as

$$R_x\left(t_{\text{peak}_{jk}}\right) = d_{jk} w_{rx_j}\left(t_{\text{peak}} + jT_b - kT_s\right) = d_{jk} A_j \left(\sum_{i=0}^{L-l_j-1} a_i^2 \right), \tag{14}$$

where a_i are the coefficients of taps of $\hat{h}(-t + jT_b - kT_s)$ and $l_j(j(T_b/\tau_s))$ are the number of taps required for a shift of jT_b. The received signal peak depends on the energy contents of $(L - l_j)$ filter coefficients. Thus, the amplitude of the received peak decreases by the sum of the squared coefficients in the shifted part of the transmitted signal.

Therefore, with the new modulation scheme, the received signal peak reduces in proportion to the energy of the shifted part of the transmitted signal.

Figure 3 shows the peak power of the received signal peak for the shifted signals normalized to the received peak with no shift. The signals are shifted by a percentage of the total number of taps in the transmitted signal. A set of 243 measured CIRs are used for the simulation. Experimental setup and the measurement procedure are explained in Section 4. The loss of the received peak power for transmitted signals corresponding to individual CIRs is represented by the dots and the dashed line is the mean of power loss. The power loss for left shift is lesser than the power loss for the right shift as the energy contained in the shifted parts of the right shift is greater than the energy contained in the shifted parts of the left shift. Although a combination of right and left shifts can be used for the communication, for the sake of simplicity we have only used left shift. In the rest of the paper unless otherwise mentioned, a shift is meant to be a left shift.

In the proposed modulation scheme, the number of shifted samples is given by $l_j = (j-1)\, l_{\text{opt}}$ where $j \in \{1, 2, \ldots, m\}$ is one of the parallel data branches and l_{opt} is the optimal shift step. The choice of the shift step (l_{opt}) is carried out under two conditions. The optimum shift step is the one which gives us an acceptable minimum signal to interference ratio (SIR) with the minimum possible shift. A minimum value of shift is required to restrict the power loss of the received peak due to the shift. Secondly, interference is introduced when multiple signals are packed in the same time slot. Thus, a shift percentage is required which gives an acceptable SIR for all the packed bits. The shift step which gives an acceptable SIR is not necessarily obtained for the large shift steps as the Signal part of the received signal decreases severely for high shift steps. Figure 4 shows the SIR for $m = 4$ with different shift steps. The figure was obtained for a measured CIR in an indoor environment. The "$*$" shows the individual SIR for different bits while the solid line shows the mean SIR. If the minimum SIR is above a certain threshold (e.g., 15 dB), the shift percentage is acceptable. We found that even the small shift steps give a satisfactory SIR performance, thus we have chosen shift steps of 2% ($0.02T_{\text{sig}}$) and 5% ($0.05T_{\text{sig}}$) in our experiments.

3.3. Theoretical Performance. To evaluate the error probability of the new modulation scheme, we suppose that the transmitted signals are quasi-orthogonal and do not result in any significant intra symbol interference. With the new proposed technique, m simultaneous bits are transmitted and each bit has energy of E_s/m. The signal space representation of the new modulation scheme consists of m dimensions. Figure 5 shows the signal space representation of the new modulation scheme for $M = 4$ ($m = 2$) and $M = 8$ ($m = 3$). $\overrightarrow{S(t)}$ represents the received signal without noise and has an energy of E_s.

The transmitted signal is a sum of m orthogonal vectors, each having an energy of E_s/m. Let the received signal vector be $\overrightarrow{X(t)} = \overrightarrow{S(t)} + \overrightarrow{N(t)}$, where $\overrightarrow{S(t)}$ is the signal vector and $\overrightarrow{N(t)}$ is the noise vector. Then the symbol error probability for the transmission system can be written as

$$P_s = 1 - P_c, \tag{15}$$

where P_c is the probability of correct decision. Let the dimensions over which the signal space diagram is represented be $x_1, x_2, \ldots, x_m$. Considering these vectors are statistically independent, the probability of the correct decision of a symbol can be written as

$$P_c = \Pr\left(\prod_{i=1}^{m} \text{Proj}\,\overrightarrow{X(t)}/x_i > 0\right) = \Pr\left(\prod \text{Proj}\,\overrightarrow{N(t)}/x_i > -\sqrt{\frac{E_s}{m}}\right), \tag{16}$$

where $\text{Proj}(\overrightarrow{\cdot})/x_i$ is the projection of $\overrightarrow{(\cdot)}$ on the dimension x_i, $\overrightarrow{X(t)}$ is the vectorial representation of the received signal, and $\overrightarrow{N(t)}$ is the noise vector. Let the projection of $\overrightarrow{N(t)}$ on the dimension x_i be represented as $p(n)$, then P_c can be written as

$$P_c = \left(\int_{-\sqrt{E_s/m}}^{+\infty} p(n)dn\right)^m = \left(1 - \frac{1}{2}\,\text{erfc}\left(\sqrt{\frac{E_s}{m\,N_0}}\right)\right)^m. \tag{17}$$

The symbol error probability can be thus written as

$$P_s = 1 - P_c \approx \frac{m}{2}\,\text{erfc}\left(\sqrt{\frac{E_s}{m\,N_0}}\right). \tag{18}$$

To find the bit error probability, from the geometrical symmetry, we can say that probabilities of error in all of the individual bits are equal and thus the average of the bit error probability is equal to the error probability of one individual bit. The bit error probability can be therefore written as

$$\begin{aligned} P_b &= \Pr\left(\text{Proj}\,\vec{N}/x_1 < -\sqrt{\frac{E_s}{m}}\right) \\ &= \int_{-\infty}^{-\sqrt{E_s/m}} p(n)dn = \frac{1}{2}\,\text{erfc}\left(\sqrt{\frac{E_s}{m\,N_0}}\right). \end{aligned} \tag{19}$$

3.4. Information Rate of the Modulation Scheme. For AWGN channel, the maximum bit rate which a system can achieve for an error-free communication is given by famous Shannon's formula for the capacity of the system:

$$C = B \log_2\left(1 + \frac{S}{N}\right), \tag{20}$$

where C is the capacity of the channel in bits per second (bps), B is the bandwidth in Hz of the transmitted signal, and S/N is the signal-to-noise ratio (SNR).

The maximum data rate for a TR scheme can also be written in a similar way. Assuming no intersymbol interference, and considering zero mean independent and identically distributed (i.i.d.) BPAM transmit symbols, the data rate can be written as

$$C = \frac{1}{T_s} \log_2\left(1 + \frac{T_s\, S}{N_0}\right), \tag{21}$$

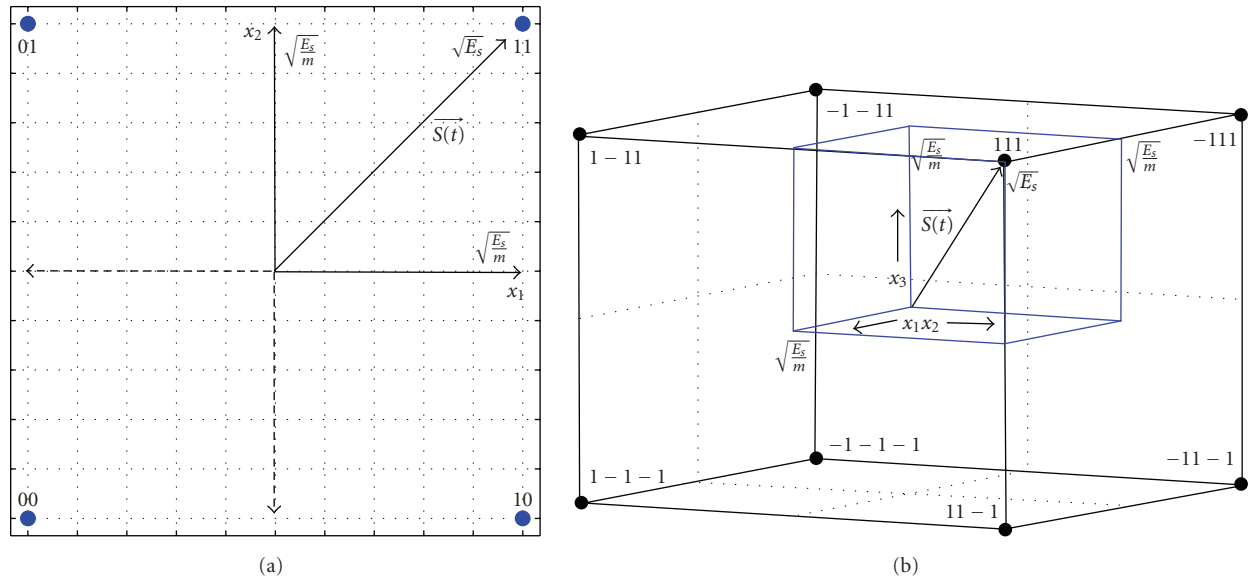

Figure 5: Signal space representation of the new modulation scheme with $M = 4$ and $M = 8$.

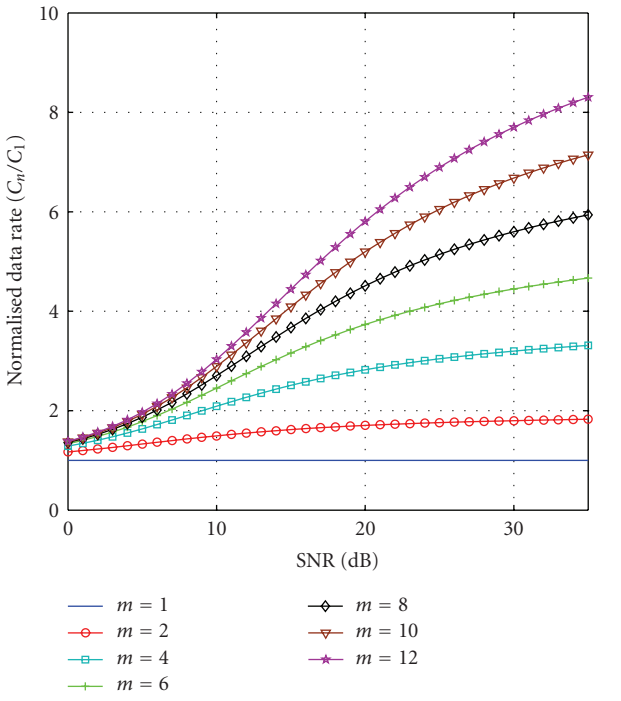

Figure 6: Data rate for m number of simultaneous bits normalized to the data rate of BPEM ($m = 1$).

where T_s is the inter symbol interval which is kept equal to the length of the truncated CIR (T_{sig}), S is the received signal peak power, and N_0 is the zero mean noise power spectral density.

The proposed modulation scheme splits the input serial data into m parallel data streams that are transmitted simultaneously by shifting the transmitted signal and packing the multiple signals in the same time slot. In this way, the system can have a sort of multiplexing gain without using any multiple antenna configuration. Thus the information rate of the proposed modulation scheme is ameliorated by factor m due to the m-parallel transmitted data in the channel. However, with the constant transmitted power P_0 for each T_s, the associated power for each transmitted data bit is reduced and the received peak signal amplitude per data bit is degraded by $1/\sqrt{m}$ and the peak signal power is degraded by $1/m$. The second degradation term is imposed by the proposed shift operation of the TR-signal samples as described in Section 3.2. Here we express the related peak signal power loss with factor k.

Another degradation factor is the interference. When multiple bits are transmitted simultaneously, there exists an interference caused by the adjacent bit within the symbol (intra symbol interference) and also there is interference in the received symbol due to the tail of the preceding symbol (inter symbol interference). As the symbols are transmitted with an inter symbol interval equal to the length of the transmitted signal ($T_s = T_{\text{sig}}$), the strength of the inter symbol interference signal is quite weak and is thus neglected. The temporal side lobes in the received signal for the adjacent bits cause the interference that reduces the system performance. This issue is reduced choosing the optimal shift step as described in the previous section. Thus for m simultaneously transmitted bits, and taking into account the k factor and the interference, (21) can be written

$$C = \frac{m}{T_s}\log_2\left(1 + \frac{1}{m}\frac{kS}{N+I}\right), \tag{22}$$

where k is the variable which takes into account the peak power loss due to the shift operation, $N = N_0/T_s$ is the noise power, and I is the intra symbol interference which depends on the shift and the temporal sidelobes of the TR received signal. The overall data rate of the given modulation scheme is increased proportionally to the number of simultaneous

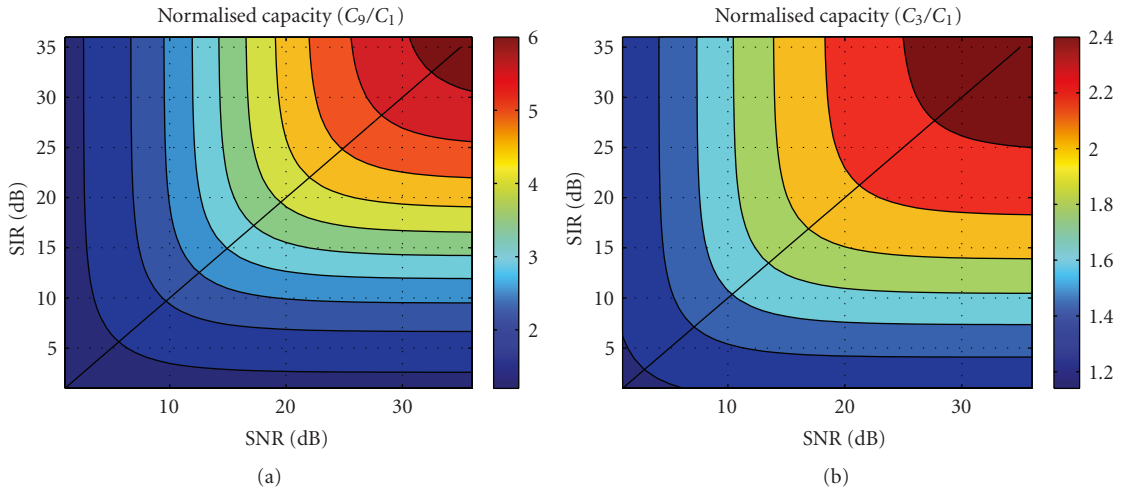

FIGURE 7: Data rate of the proposed modulation scheme against both SNR and SIR normalized to the data rate of $m = 1$ for (a) $m = 9$ (b) $m = 3$.

bits (m) and the degradation terms are varied by the logarithmic function with k, I and $1/m$. If the interference is neglected ($I = 0$) and k is kept close to unity, that is, the optimum performance of the modulation scheme is considered, the maximum data rate of the modulation scheme is simplified as

$$C_{\text{ideal}} = \frac{m}{T_s} \log_2\left(1 + \frac{1}{m}\frac{S}{N}\right). \tag{23}$$

Figure 6 shows the data rate for a different number of simultaneous transmitted bits (m) normalized to the data rate for a BPAM transmitted signal ($m = 1$). For each value of SNR, the data rate for a given m is normalized to the corresponding data rate of a BPAM signal ($m = 1$). It shows that with the new modulation scheme, the data rate increases significantly with m for a constant SNR specially for high SNR. For instance, for an SNR of 20 dB, the data rate increases by a factor of 2.82 for $m = 4$, 4.51 for $m = 8$, and 5.19 for $m = 10$.

Figure 7 shows, for $m = 3$ and $m = 9$, the maximum achievable data rate normalized to the data rate for a BPAM transmitted signal ($m = 1$) against both SNR and SIR. Thus, the effects of ISI are included in this figure. The power loss due to the shift operation is neglected, that is, $k = 1$, thus the data rate is given by (22) with $k = 1$. It shows that an optimal performance is achieved at SIR $\geq$ SNR.

4. Experimental and Simulative Validation of the New Modulation Scheme

To analyze the bit error rate performance of the new modulation scheme, two separate measurement campaigns are performed for two different typical indoor environments. Two different environments are chosen to include more generality in the results.

4.1. Measurement Campaign 1. In the first measurement campaign, the frequency responses are measured for varying positions of the receiver over a rectangular surface of 65 cm × 40 cm. A vector network analyzer (VNA) is used to measure the frequency responses. Thereafter, a TR communication is simulated and the BER performance of the new modulation scheme is analyzed.

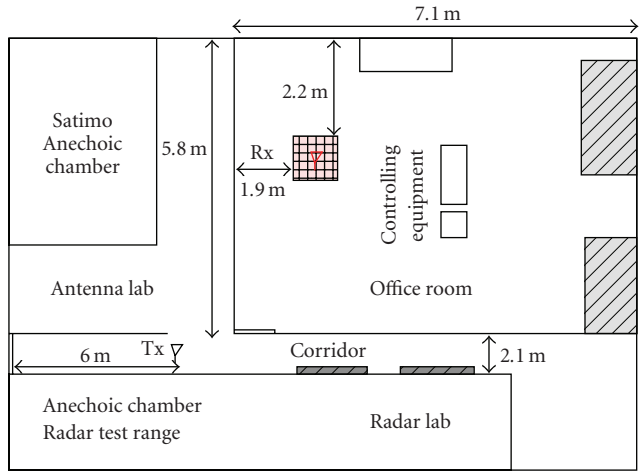

FIGURE 8: Environment layout of the first measurement cappaign.

4.1.1. Experimental Setup. Experiments are performed in a typical indoor environment. The environment is an office space of 14 m × 8 m in the IETR laboratory. Figure 8 shows the environment layout of the first measurement campaign. The frequency responses of the channel in the frequency range of 0.7–6 GHz are measured using a VNA with a frequency resolution of 3.3 MHz. Two wide-band conical mono-pole antennas (CMA) are used in a nonline of sight (NLOS) configuration. The height of the transmitting and the receiving antennas is 1.5 m from the floor. The receiver is moved over a rectangular surface (65 cm × 40 cm) with a precise positioner system. Respective spatial resolution

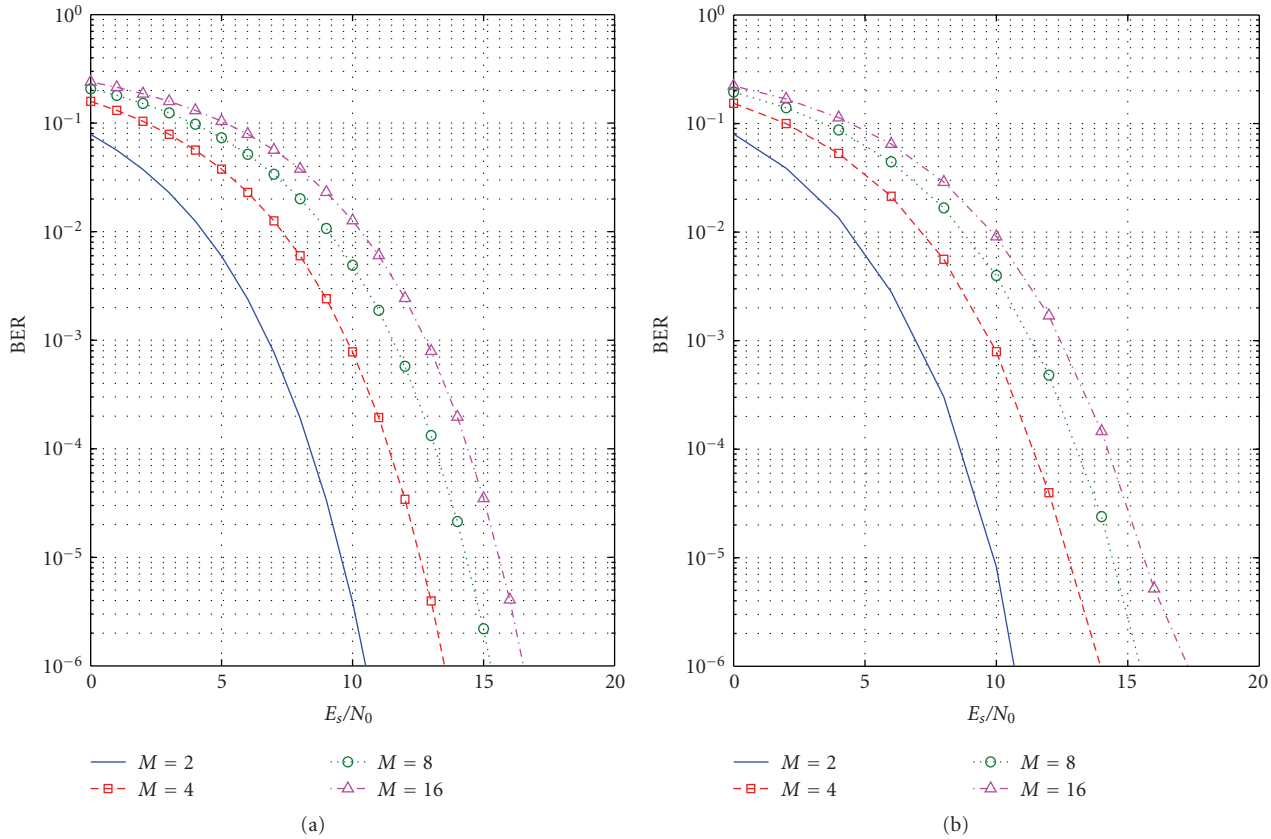

FIGURE 9: BER performance of the new modulation scheme for different modulation orders. (a) Theoretical curves (b) simulated curves with a shift step of $0.02T_{\text{sig}}$.

of 2.5 cm and 5 cm is used for the x-axis and y-axis of the horizontal plane. Thus 243 (27×9) measurements are taken over the rectangular surface. The frequency responses between the transmitting antenna and receiving virtual array (of 243 antennas) are measured. The time domain CIRs are computed using the inverse fast Fourier transformation (IFFT) of the measured frequency responses.

4.1.2. BER Performance. The BER performance of the system is evaluated for different number of simultaneously transmitted bits. In the simulations, for each measured channel, 500000 symbols are transmitted to have enough data for statistical analysis.

Ideal theoretical curves for the new modulation scheme for multiple number of simultaneously transmitted bits (from (19)) are plotted in Figure 9(a), and Figure 9(b) shows the simulative BER performance of the proposed modulation scheme for different modulation orders. A shift step of 2% of the length of the transmitted signal ($0.02\ T_{\text{sig}}$) is kept and only left shift is used. The performance of the new modulation scheme is in strong agreement with the theoretical BER performance. A small shift percentage enabled a negligible loss in the received peak power, and quasi-othogonal transmitted signals resulted in a very low intra symbol interference. It must be noted that the proposed modulation scheme gives a better performance than M-ary quadrature amplitude modulation (QAM) and PAM for $M \geq 4$. The theoretical performance of the error probability of these modulation schemes can be found in [18]. Figure 10 shows the curves for the QAM and PAM modulation schemes in an AWGN channel for $2 \leq M \leq 16$. Comparing Figures 9 and 10, it can be seen that the proposed modulation scheme performs better than QAM and significantly better than PAM. For instance, for $M = 4$, the proposed modulation scheme gives similar performance to QAM, but 3.88 dB better performance than PAM for a fixed BER of 10^{-6}. For higher modulation orders, the proposed modulation scheme even outperforms the QAM. For instance, for $M = 16$, the proposed modulation scheme gives a 3.89 dB and 13 dB better performance than QAM and PAM, respectively, for a fixed BER of 10^{-6}.

It is interesting to note that for the new modulation scheme, bit energy-to-noise ratio, E_b/N_0 , remains almost constant for all M for a given BER. Therefore, symbol energy-to-noise ratio, E_s/N_0, follows the following equation:

$$\frac{E_s}{N_0}(\text{dB}) = \frac{E_b}{N_0}(\text{dB}) + 10\log_{10}(\text{m}), \tag{24}$$

where E_b/N_0 is the bit energy-to-noise ratio. For instance, for a fixed BER of 10^{-5}, $E_s/N_0 = 10$ dB for $M = 2$. Same BER is achieved for an E_s/N_0 of 16 dB for $M = 16$. These results are in agreement with (24). Therefore, with the new

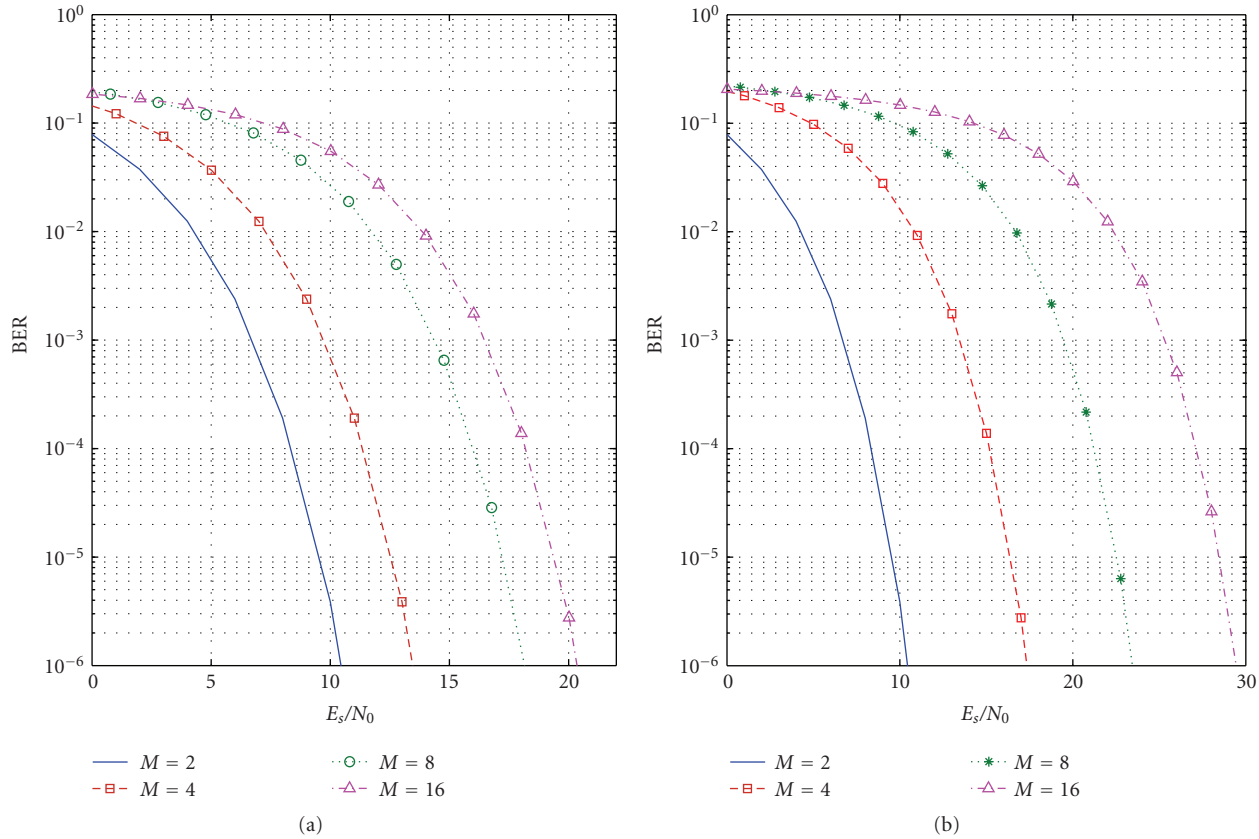

Figure 10: BER performance for different modulation orders in the AWGN channel for (a) QAM (b) PAM.

modulation scheme, the data rate is increased linearly while the E_s/N_0 increases in proportion to the log term (24). This performance is only achieved for a small shift step. For higher shift steps, as we will see, the performance is not the same.

If a higher shift step is chosen, the power loss due to shift also affects the performance of the system. Figure 11 shows the simulative BER performance of the system with a shift step of 5% ($0.05T_{\text{sig}}$). The effect of the power loss due to the shift is evident on the performance of the system. For example, for a fixed BER of 10^{-5} and $M = 16$, a 2 dB degradation is observed with higher shift step of $0.05T_{\text{sig}}$ compared to the lower shift step of $0.02T_{\text{sig}}$ (see Figures 11 and 9(b)).

4.2. Measurement Campaign 2. A time domain validation of the new modulation scheme is performed by making use of time domain instruments: an arbitrary waveform generator (Tektronix AWG 7052) and a high-speed digital storage oscilloscope (Tektronix DSO 6124C). For this purpose, a second measurement campaign is carried out in another typical indoor environment. The environment also has a reverberation chamber which increases the number of multipaths at the receiver. In this case, the performance of the new modulation scheme is experimentally studied.

4.2.1. Experimental Setup. An experimental setup is established in a typical indoor environment (laboratory IETR) having the plan shown in Figure 12. All rooms are furnished with office equipments: tables, PCs, and seats. Moreover, there is a large reverberating chamber in the laboratory, which increases the wave reflections in the environment. Two Conical Mono-pole Antennas (CMA) are used as the transmitter and the receiver. The distance between the transmitter and the receiver is 8.5 m while the height is 1 m from the ground. The pulse is generated with an Arbitrary Waveform Generator (AWG 7052), which has a maximum sampling rate of 5 GS/s. At the receiver end, the signals are captured by a Digital Storage Oscilloscope (Tektronix DSO 6124C) with a maximum sampling rate of 40 GS/s. The experimental setup is shown in Figure 13.

Once the CIR is measured, 1000 transmitted symbols for different modulation orders are created through MATLAB and are retransmitted in the same channel. A left shift percentage of 5% is kept for each M. The DSO is operated in average mode and the received signal is averaged 256 times so that the effects of the noise are compensated. Figure 14 shows for $M = 16$, 3 consecutive frames of the measured received signal with the new modulation scheme detected through the DSO. All five peaks inside a time slot can easily be detected.

4.2.2. BER Performance. To analyze the BER performance of the modulation scheme validated by the experiments, random noise is added in the received signal and the experiment is repeated in order to reach 10^8 transmitted bits

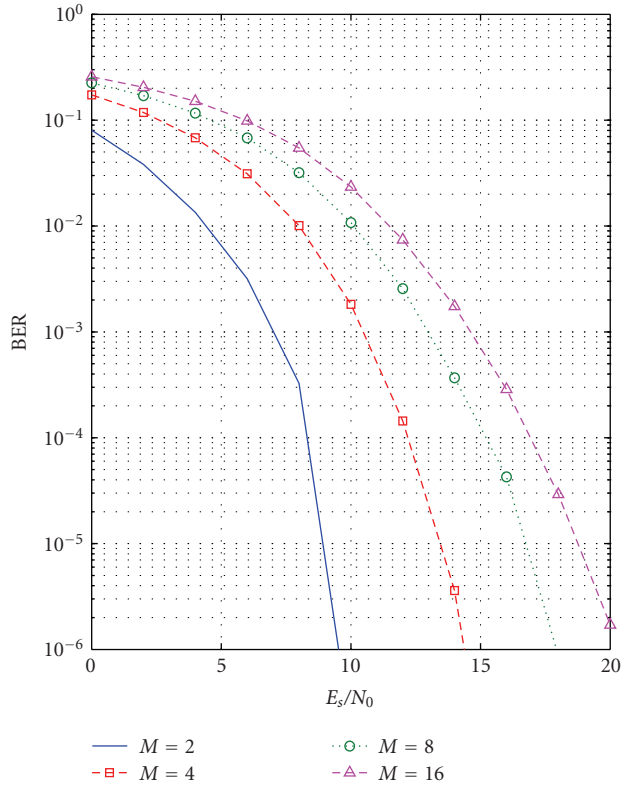

Figure 11: Simulative BER performance of the new modulation scheme for different modulation orders with a shift step of $0.05T_{sig}$.

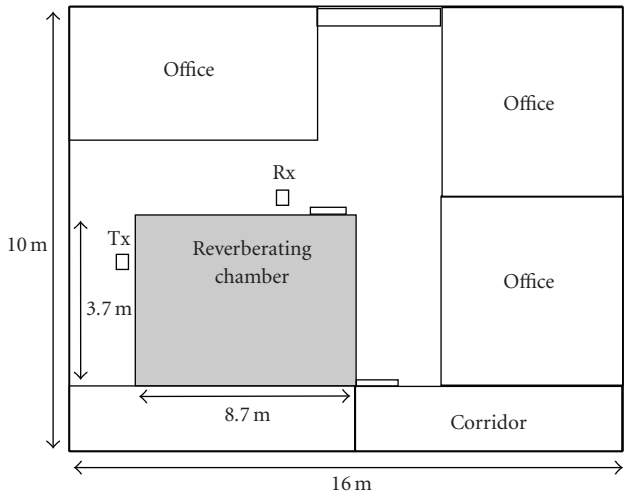

Figure 12: Measurement environment layout of the measurement campaign 2.

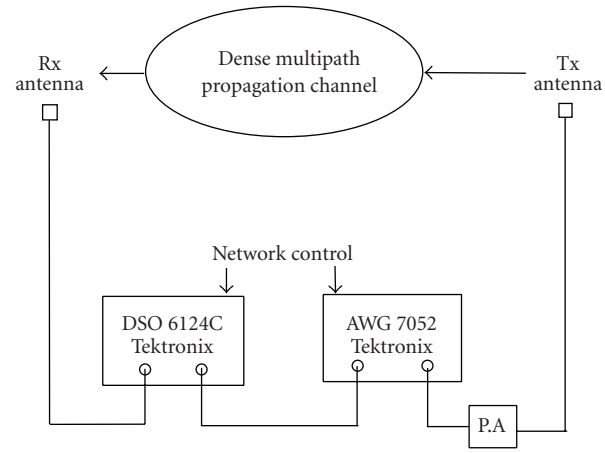

Figure 13: Experimental Setup of the measurement campaign 2.

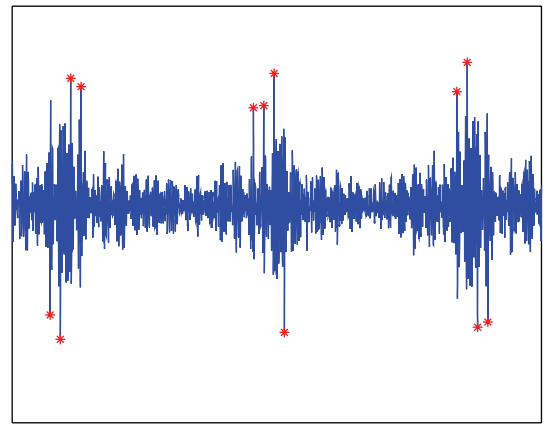

Figure 14: Received signal for $M = 16$ with the new modulation scheme.

for each M. Figure 15 shows the BER performance of the new modulation scheme using the experimental results of measurement campaign 2 for different M. The performance of the modulation scheme with measurement campaign 2 is in good agreement with the performance with the results of measurement campaign 1 for a shift step of $0.05T_{sig}$ (see Figures 11 and 15). Even though the two measurement campaigns are carried in two different environments, their performances match with good agreement. The performance can never match exactly as the curves for measurement campaign 1 are achieved by simulating the TR communication for a set of 243 measured CIR while the performance of the campaign 2 is carried out for over one single channel. Furthermore, the time domain equipments are subjected to the inherent jitter which may reduce the received signal peak and may cause the degradation of the performance.

5. Conclusion

In this paper, a new modulation scheme is proposed for a time reversal (TR) ultra wide-band (UWB) communication system. The proposed modulation scheme adds a new level of modulation to the existing modulation scheme like bipolar pulse amplitude modulation (BPAM). Multiple bits are transmitted simultaneously by shifting the transmitted signal and packing them in the same time slot. The BER performance of the new modulation scheme is theoretically studied. Thereafter, it is shown that for negligible interference and quasi orthogonal signals, the data rate of the modulation scheme increases linearly whereas the transmitted power must only be increased logarithmically.

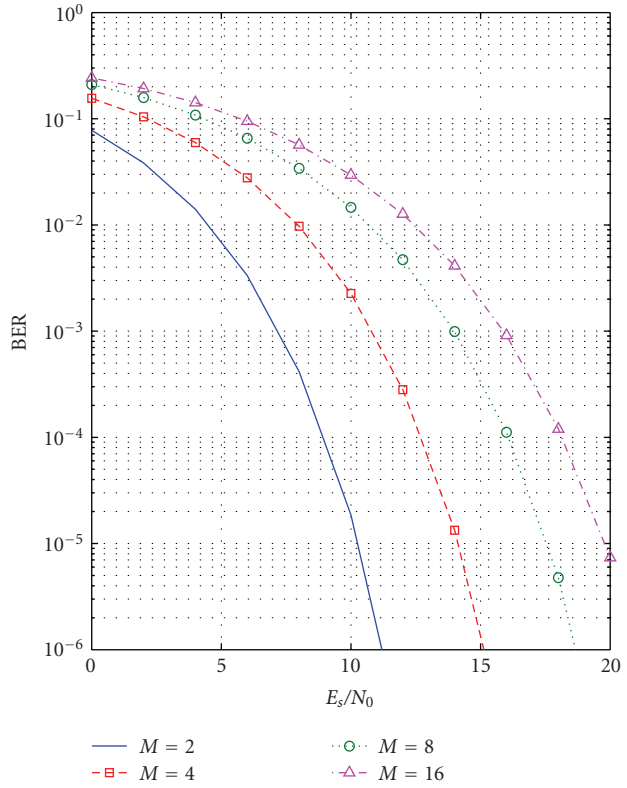

FIGURE 15: BER performance of the new modulation scheme for different modulation orders with using the experimental results of measurement campaign 2.

The validation of the modulation scheme is carried out with the help of two separate measurement campaigns. For the first measurement campaign, the frequency responses of a typical indoor channel are measured with a vector network analyzer and TR communication is simulated for the new modulation scheme. The bit error rate performance of the new modulation scheme is analyzed for different modulation orders. It is shown that for an optimal shift, theoretical and simulative performances of the modulation scheme are in strong agreement with each other. In the second measurement campaign, time domain instruments are used to measure the channel impulse response and the new modulation scheme is validated experimentally. It is shown that the experimental and the simulative results are in good agreement with each other.

Acknowledgments

This work was supported by ANR project MIRTEC and French research ministry.

References

[1] R. Hoctor and H. Tomlinson, "Delay-hopped transmitted-reference RF communications," in *Proceedings of the 2nd IEEE Ultra Wideband Systems and Technologies (UWBST '02)*, pp. 265–269, Baltimore, Md, USA, May 2002.

[2] R. J. Fontana, E. Richley, and J. Barney, "Commercialization of an Ultra Wideband Precision Asset Location system," in *Proceedings of the IEEE Conference UWB systems and Technologies*, Reston, Va, USA, 2003.

[3] J. D. Choi and W. E. Stark, "Performance of ultra-wideband communications with suboptimal receivers in multipath channels," *IEEE Journal on Selected Areas in Communications*, vol. 20, no. 9, pp. 1754–1766, 2002.

[4] M. Fink, "Time-reversed acoustic," *Scientific American*, pp. 67–73, November 1999.

[5] A. Derode, A. Tourin, J. De Rosny, M. Tanter, S. Yon, and M. Fink, "Taking advantage of multiple scattering to communicate with time-reversal antennas," *Physical Review Letters*, vol. 90, no. 1, Article ID 014301, 4 pages, 2003.

[6] H. T. Nguyen, I. Z. Kovcs, and P. C. F. Eggers, "A time reversal transmission approach for multiuser UWB communications," *IEEE Transactions On Antennas and Propagation*, vol. 54, no. 11, 2006.

[7] P. Kyritsi, G. Papanicolaou, P. Eggers, and A. Oprea, "MISO time reversal and delay-spread compression for FWA channels at 5 GHz," *IEEE Antennas and Wireless Propagation Letters*, vol. 3, no. 1, pp. 96–99, 2004.

[8] P. Kyritsi and G. Papanicolaou, "One-bit time reversal for WLAN applications," in *Proceedings of the 16th IEEE International Symposium on Personal, Indoor and Mobile Radio Communications (PIMRC '05)*, vol. 1, pp. 532–536, Berlin, Germany, September 2005.

[9] A. E. Akogun, R. C. Qiu, and N. Guo, "Demonstrating time reversal in ultra-wideband communications using time domain measurements," in *Proceedings of the 51st International Instrumentation Symposium*, Knoxville, Tenn, USA, May 2005.

[10] C. Oestges, J. Hansen, S. M. Emami, A. D. Kim, G. Papanicolaou, and A. J. Paulraj, "Time reversal techniques for broadband wireless. Communication systems," in *Proceedings of the European Microwave Conference*, pp. 49–66, Amsterdam, The Netherlands, October 2004.

[11] H. T. Nguyen, J. B. Andersen, and G. F. Pedersen, "The potential use of time reversal techniques in multiple element antenna systems," *IEEE Communications Letters*, vol. 9, no. 1, pp. 40–42, 2005.

[12] T. Strohmer, M. Emami, J. Hansen, G. Papanicolaou, and A. J. Paulraj, "Application of time-reversal with MMSE equalizer to UWB communications," in *Proceedings of the IEEE Global Telecommunications Conference (GLOBECOM '04)*, vol. 5, pp. 3123–3127, Dallas, Tex, USA, November-December 2004.

[13] R. C. Qiu, C. Zhou, N. Guo, and J. Q. Zhang, "Time reversal with miso for ultra-wideband communications: experimental results," in *Proceedings of the IEEE Radio and Wireless Propagation Letters Symposium*, pp. 499–502, San Diego, Calif, USA, January 2006.

[14] A. Khaleghi, G. El Zein, and I. H. Naqvi, "Demonstration of time-reversal in indoor ultra-wideband communication: time domain measurement," in *Proceedings of the 4th IEEE Internatilonal Symposium on Wireless Communication Systems (ISWCS '07)*, pp. 465–468, Trondheim, Norway, October 2007.

[15] A. Khaleghi and G. El Zein, "Signal frequency and bandwidth effects on the performance of UWB time-reversal technique," in *Proceedings of the Loughborough Antennas and Propagation Conference (LAPC '07)*, pp. 97–100, Loughborough, UK, April 2007.

[16] I. H. Naqvi, A. Khaleghi, and G. Elzein, "Performance enhancement of multiuser time reversal UWB communication system," in *Proceedings of the 4th IEEE Internatilonal*

Symposium on Wireless Communication Systems (ISWCS '07), pp. 567–571, Trondheim, Norway, October 2007.

[17] A. Khaleghi and G. El Zein, "Procédé de modulation pour les communications sans fil à retournement temporel," Brevet Franais d'Invention, Bretagne Valorisation, September 2007.

[18] J. G. Proakis, *Digital Communications*, McGraw-Hill, New York, NY, USA, 4th edition, 2001.